Jinst

14TH TOPICAL SEMINAR ON INNOVATIVE PARTICLE AND RADIATION DETECTORS
3–6 OCTOBER 2016
SIENA, ITALY

High Luminosity LHC: challenges and plans

G. Arduini,[a] J. Barranco,[a] A. Bertarelli,[a] N. Biancacci,[a] R. Bruce,[a] O. Brüning,[a] X. Buffat,[a] Y. Cai,[b] L.R. Carver,[a] S. Fartoukh,[a] M. Giovannozzi,[a,1] G. Iadarola,[a] K. Li,[a] A. Lechner,[a] L. Medina Medrano,[a] E. Métral,[a] Y. Nosochkov,[b] Y. Papaphilippou,[a] D. Pellegrini,[a] T. Pieloni,[a] J. Qiang,[c] S. Redaelli,[a] A. Romano,[a] L. Rossi,[a] G. Rumolo,[a] B. Salvant,[a] M. Schenk,[a] C. Tambasco,[a] R. Tomás,[a] S. Valishev[d] and F.F. Van der Veken[a]

[a]*Accelerator and Technology Sector, CERN,*
 385 Route de Meyrin, 1217 Meyrin, Switzerland

[b]*Accelerator Research Division, SLAC National Accelerator Laboratory,*
 2575 Sand Hill Road Menlo Park, CA 94025-7015, U.S.A.

[c]*Accelerator Technology and Applied Physics Division, Laurence Berkeley National Laboratory,*
 1 Cyclotron Road, Berkeley, CA 94720, U.S.A.

[d]*Accelerator Division, Fermilab,*
 PO Box 500, Batavia IL 60510-5011, U.S.A.

 E-mail: massimo.giovannozzi@cern.ch

ABSTRACT: The Large Hadron Collider (LHC) is one of the largest scientific instruments ever built. Since opening up a new energy frontier for exploration in 2010, it has gathered a global user community working in fundamental particle physics and the physics of hadronic matter at extreme temperature and density. To sustain and extend its discovery potential, the LHC will undergo a major upgrade in the 2020s. This will increase its rate of collisions by a factor of five beyond the original design value and the integrated luminosity by a factor ten. The new configuration, known as High Luminosity LHC (HL-LHC), will rely on a number of key innovations that push accelerator technology beyond its present limits. Among these are cutting-edge $11 - 12$ T superconducting magnets, including Nb_3Sn-based magnets never used in accelerators before, compact superconducting cavities for longitudinal beam rotation, new technology and physical processes for beam collimation. The dynamics of the HL-LHC beams will be also particularly challenging and this aspect is the main focus of this paper.

KEYWORDS: Accelerator Subsystems and Technologies; Beam dynamics

---

[1]Corresponding author.

Contents

1 Goals of the high luminosity upgrade

The Large Hadron Collider (LHC, see ref. [1] for more detail) was successfully commissioned in 2010 for proton-proton collisions with a 7 TeV centre-of-mass energy. It delivered 8 TeV centre-of-mass proton collisions from April 2012 until the end of Run 1 in 2013. Following the first long shut down (LS1) in 2013-2014, it operated with 13 TeV centre-of-mass proton collisions during Run 2 from 2015 onwards.

To enhance its discovery potential, the LHC will need a major upgrade in the 2020s to extend its operability by another decade and to increase its luminosity, and thus collision rate, by a factor of five beyond its design value.

The instantaneous luminosity L, which is the key figure of merit for a collider, is given by

$$L = \frac{n_b N^2 f_{\mathrm{rev}} \gamma_{\mathrm{rel}}}{4\pi \beta^* \epsilon_n} R\left(\beta^*, \sigma_z, d_{\mathrm{bb}}\right) . \tag{1.1}$$

The r.m.s. normalized emittance ϵ_n in collision is assumed here to be equal for the two beams and for the horizontal and vertical planes. The r.m.s. beam size at the interaction point (IP) is given by $\sigma^* = \sqrt{\epsilon_n \beta^*/\gamma_{\mathrm{rel}}}$ where β^* is the optical beta-function, γ_{rel} is the relativistic gamma factor and the relativistic β_{rel} is always assumed to be unity. A crossing angle is needed to separate bunches immediately upstream and downstream of the collision point. This ensures a sufficient long-range beam-beam separation d_{bb}, but also reduces the geometric overlap between the colliding beams, thus reducing L. The luminosity is also reduced by the 'hourglass effect' that arises from the increase of the beta function along the bunch longitudinal distribution, and the factor R in eq. (1.1) takes both the crossing angle and the hourglass effect into account. The considerations that constrain the values of all these parameters are reviewed in refs. [2–4], where the main two goals of the HL-LHC project are also discussed:
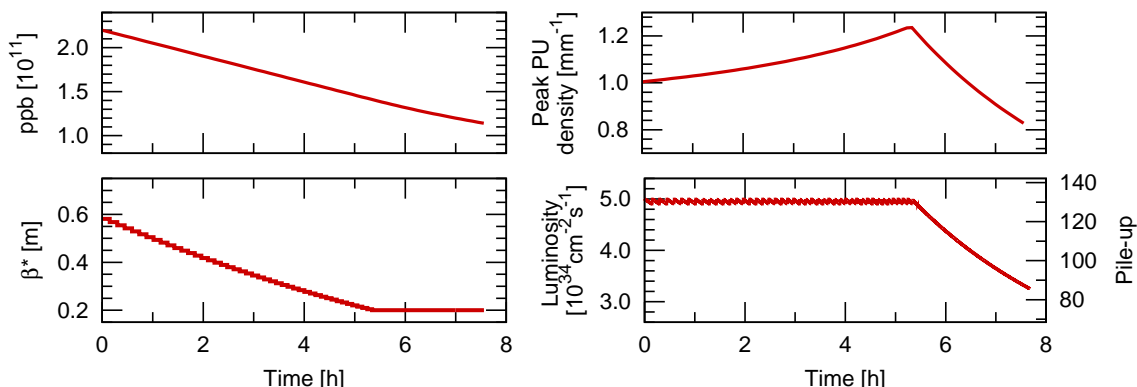
Figure 1. Simulated evolution of main beam parameters during a nominal HL-LHC physics fill.

- a peak luminosity in ATLAS and CMS of 5×10^{34} cm^{-2}s^{-1} sustained over several hours using luminosity levelling techniques compatibly with a maximum average pile-up, i.e. the number of events per bunch crossing, limit of 140 events/bunch crossing defined by the experiments;

- an average integrated luminosity of 250 fb^{-1} per year with the goal of 3000 fb^{-1} in about a dozen years after the upgrade.

It is expected that the engineering margin applied in the design of the accelerator components should allow to operate the machine up to a peak levelled luminosity of about 7.5×10^{34} cm^{-2}s^{-1} increasing the average pile-up in the detectors up to around 200. This luminosity should enable the collection of up to about 4000 fb^{-1} during the HL-LHC lifetime assuming an higher performance efficiency close to 60 % as it has been achieved during the LHC operation in 2016.

Radio frequency deflectors, called crab cavities, first proposed in 1988 as a means to increase the luminosity of linear colliders, then installed in the B-factory KEKB in 2007, but never used in hadron machines, will be used in the interaction regions to increase the overlap between the colliding beams, hence increasing the virtual[1] luminosity, allowing to level over sufficiently long periods and to decrease pile-up density. To note that the crab cavity voltage is not sufficient to fully compensate for the crossing angle. Baseline parameters are presented in table 1, while a simulated HL-LHC physics fill is shown in figure 1. Details of the simulation are described in [5]. The saw-tooth pattern in the instantaneous luminosity reflects the step-wise changes in β^* to restore luminosity after a 2 % decay. In this configuration the 250 fb^{-1} are achieved in 160 days with 52 % efficiency during Run 4. This value will increase in the following years due to the increase of the number of days of operation, resulting from the stop of the ion operation after Run 4, and a reduction of the machine studies required for performance enhancement.

Improvements to the HL-LHC baseline are currently being explored, including new filling schemes and further reduction of β^* and crossing angle.

For the sake of completeness it is worth mentioning that the HL-LHC physics programme includes ions physics, too (see e.g., refs. [3, 4] for more detail).

---

[1]This term refers to the peak luminosity without levelling.

Table 1. Main IP and beam parameters for the HL-LHC baseline scenario.

E [TeV]	7
Particles per bunch [10^{11}]	2.2
Number of bunches	2748
IP1 and 5 collisions	2736
Beam current [A]	1.09
Crossing angle [μrad]	510
beam separation [σ]	12.5
β^* [cm]	20
ϵ_n [μm]	2.5
ϵ_L [eVs]	3
Relative E spread [10^{-4}]	1.18
r.m.s. bunch length [cm]	9
Crabbing angle [μrad]	380
Virtual luminosity [10^{35}cm^{-2}s^{-1}]	1.17

2 Layout and optics

The HL-LHC layout is based on the nominal LHC ring configuration, in which about 1.2 km of beam line will be changed. The nominal configuration is designed for a realistic, cost-efficient and achromatic implementation of low β^* collision optics, based on the deployment of the Achromatic Telescopic Squeeze (ATS) scheme [6], together with the installation of insertion magnets of larger aperture [2, 3]. The first successful validation tests of ATS with beam were achieved in 2011-2012 [7] in very specific conditions, and more recently in additional machine studies in 2016.

In figure 2 the layout of the new high-luminosity insertion regions (IR) is shown (upper part), while in the lower part the evolution of the beta function along the insertion is plotted.

The single-aperture magnets, namely the triplet quadrupoles — Q1, Q2a, Q2b, Q3 — for strong beam focusing at the IP and the separation dipole D1, are visible close to the IP side of the insertion. The two-in-one apertures magnets, the separation dipole D2 and the quadrupole Q4, are also shown. The large mechanical aperture of insertion magnets is needed to accommodate the beams, which reach large dimensions (note the peak value of the beta functions in excess of 20 km), including also appropriate layers of tungsten to protect the superconducting magnets from the collision debris.

Additional protection is ensured by a number of fixed absorbers (TAXS, TAXN) and movable devices (TCLX).

The crab cavities are integrated in the same region and provide an essential contribution to HL-LHC performance. In fact, by rotating along the longitudinal axis the bunches upstream and downstream of the IP, they increase the value of the factor R in eq. (1.1).

The changes in some of the dispersion suppressors in view of the upgrade of the collimation system are mentioned in section 3.4.
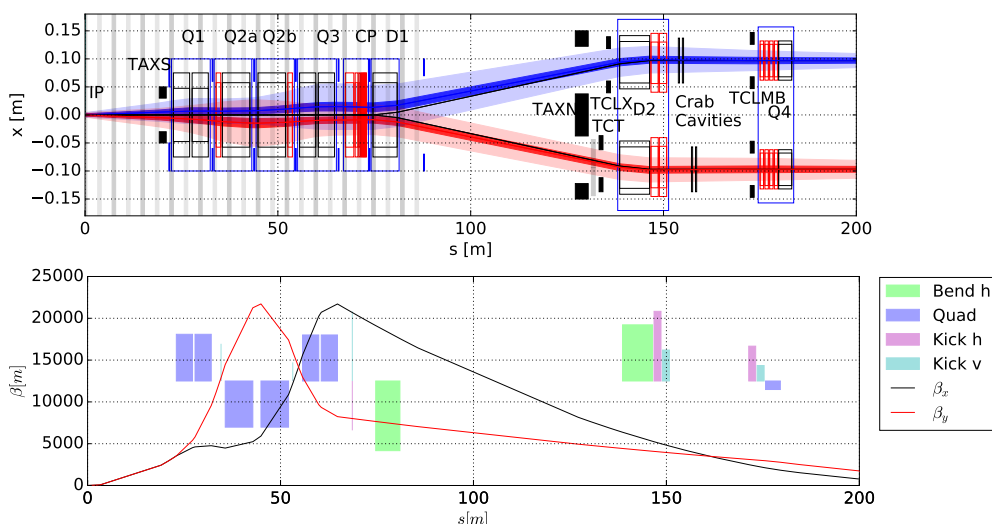
Figure 2. Upper: overall layout of one side of the insertion region between the IP and Q4 in Point 1 and 5. The dark blue and red areas represent the 2.4 σ beam envelope for the nominal round optics. The light regions correspond to a 14.2 σ value of the beam envelope. The vertical, shaded grey areas represent the locations of the parasitic beam-beam encounters. Lower: evolution of the beta function in the insertion region.

3 Main challenges

3.1 Beam stability

Transverse instabilities have been observed in the LHC in Run 1, with 50 ns beams, and in Run 2, with 25 ns beams, and have required operating the machine with high chromaticity ($Q' \approx +15$) and Landau octupole strength close to the maximum feasible, and with maximum gain and bandwidth of the transverse feedback (50 turns and 20 MHz, respectively) [8]. The observations have clearly evidenced that in several cases the observed instabilities are the result of the interplay of various mechanisms. Indeed, the impact on beam stability of coupling impedance, electron cloud, head-on and long-range beam-beam forces, realistic models of transverse feedback, machine optical parameters such as tunes, linear coupling, linear and non-linear chromaticity, and other non-linear effects, is currently under study.

During 2015 and 2016, systematic measurements with single-bunch beams of the LHC impedance showed a good agreement between the expected stabilising current of Landau octupoles and the measured values as a function of chromaticity.

Given the higher bunch population and beam brightness expected for HL-LHC and the fact that almost the maximum values in chromaticity and Landau octupole current have been used since 2012, the transverse impedance should be kept under control by reducing the impedance of existing components and minimising that of new components, in particular of the devices installed in regions with high beta functions like the crab cavities. This is pursued by a vigorous upgrade programme of the collimation system as, according to the present estimates, there is no sufficient margin for HL-LHC beam stability with the present primary and secondary collimators in IR7 that have to be changed with a low-impedance design (see section 3.4). Moreover, the negative current in the Landau octupoles was chosen after a detailed analysis of the interplay between octupoles
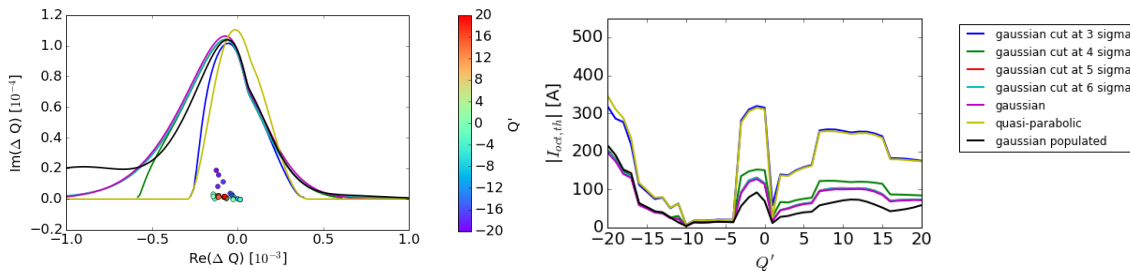
Figure 3. Effects of the tails of the transverse beam profiles on the single-beam stability just before putting beams in collision with the current HL-LHC impedance model: (left) stability diagram with the coherent modes inside and (right) required Landau octupoles current vs. chromaticity to reach beam stability.

and beam-beam long range during the optics squeeze process. The corresponding stability diagram and coherent modes just before putting beams in collision are shown in figure 3 (left) for different transverse beam distributions to probe the effect of the tails, while the required Landau octupole current to stabilize the beam vs. chromaticity is shown in figure 3 (right) [9]. It can be seen that the beam is stable in all cases if the current in the Landau octupoles is larger than about half the maximum value, thanks to the efforts to reduce collimators impedance and crab cavities high-order modes.

The operation with 25 ns beam relies heavily on beam-induced scrubbing. The full electron cloud suppression should be possible for the arc dipoles, but it still needs to be confirmed, whereas it seems very unlikely for the quadrupoles. Coherent beam instabilities are currently observed at injection in the presence of electron cloud, which require to use high values of chromaticity ($Q' \approx +20$ units) in both planes, high transverse damper gain (damping times of ≈ 10 turns) and high Landau octupole strength. Simulation studies are on going to assess whether the observed instabilities are generated only by electron cloud or if some interplay between different mechanisms is involved. As a result of the experience gained in 2015 and 2016 the definition of the working point for HL-LHC has further progressed: it is proposed to operate HL-LHC at injection with the horizontal and vertical fractional tunes 0.27/0.295 instead of the nominal values 0.28/0.31 and to compensate automatically the Laslett tune shifts during the injection process. This will allow accommodating the large tune spread created by the high Q' and large strength of the Landau octupoles needed to stabilize the beam against electron cloud; as linear coupling can drive the beam unstable because of loss of transverse Landau damping, special care should be paid to its measurement and correction, or alternatively the separation of the tunes should be increased.

Other mitigation measures under study are the introduction of a larger transverse tune spread for Landau damping using second order chromaticity or a RFQ [10], or the suppression of the intra-bunch motion by a wide-band feedback system [11], which could be of interest in case of instabilities resulting from electron cloud.

Longitudinal instabilities are not expected to be a major issue for the HL-LHC, thanks to the choice of the nominal bunch length of 9 cm (see table 1), as shorter bunches might indeed become unstable.

3.2 Beam-beam effects

The beam-beam interaction is known to be an important factor limiting the performance of colliders, including the LHC and its high-luminosity upgrade. A combination of mechanisms such as resonance crossing due to large beam-beam tune-spread coupled with magnetic imperfections and noise effects can degrade the beam quality inducing losses and/or emittance blow-up. This decreases beam and luminosity lifetime generating also high background for physics experiments, heat and radiation load on collimation system.

The beam-beam effects in the LHC were extensively studied during its design phase [12, 13]. A number of experiments were recently undertaken proving that the present LHC has surpassed the head-on beam-beam tune-shift limit, which was assumed based on experience from past colliders [12]. However, the HL-LHC represents a quantitative and qualitative leap into unknown territory. The baseline configuration employs novel concepts, such as luminosity leveling by variation of the β^*, tilting bunches in the main IPs with crab cavities, significantly higher head-on beam-beam tune shift: all these require careful verification.

The beam-beam studies for HL-LHC are mostly performed using the weak-strong approximation and employ different tracking codes [13, 14] capable of calculating the area of stable motion in phase space, also called dynamic aperture (DA), over a few million turns (i.e. a few minutes). Where necessary, strong-strong simulations are also performed [15–19]. The criterion used for establishing satisfactory beam dynamics behavior is similar to that of the LHC design, with a target DA value of 6 σ for 10^6 turns and HL-LHC baseline parameters. The DA target value is currently under scrutiny and an effort is on going to complement DA calculations with multiparticle simulations, which are slower to compute, but produce directly measurable quantities [20, 21].

Weak-strong beam-beam simulations confirmed that the target DA is achieved and surpassed during the whole leveling process [3], which gives confidence that also for the ultimate scenario there is adequate margin, either for reducing the crossing angle or for accommodating the impact of non-linearities, such as magnetic multipole imperfections, high chromaticity, and Landau octupoles. A global exploration of the impact on DA of all the related parameters, including possible compensation of the long-range beam-beam effects for non-baseline scenarios [22], are under study for refining operational scenarios and optimising the projected HL-LHC performance. An example is seen in figure 4 where the DA is shown vs crossing angle and bunch charge.

Weak-strong simulations were also used to evaluate the emittance growth due to beam-beam-related betatron resonances, predicting that the corresponding luminosity lifetime will be large [20, 21, 23]. Another mechanism of emittance degradation can be due to the interplay between the non-linear beam-beam interaction and various sources of noise. These effects require strong-strong simulations and the key results are found in refs. [15, 19]

3.3 Beam-induced heat load on the cryogenic system

The circulating beam can deposit a significant amount of power on the structures exposed to it mainly through three mechanisms: synchrotron radiation, impedance, and electron cloud.

Synchrotron radiation is the most important contribution to the heat load on beam screens in the arcs, which amounts to 0.66 W/m/beam, assuming nominal HL-LHC parameters, whereas the longitudinal beam screen impedance generates additional 0.47 W/m/beam. The remaining
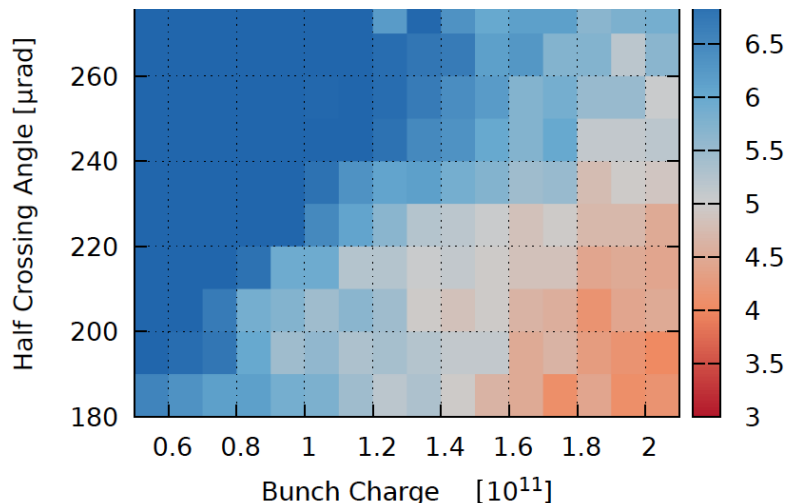
Figure 4. Minimum DA vs. crossing angle and bunch charge for $\beta^* = 0.2$ m, $Q' = 3$, and maximum strength of the Landau octupoles. The bunch charge is in the range typical of a nominal HL-LHC fill (see figure 1).

contribution from electron cloud effects depends on the Secondary Electron Yield (SEY) of the beam screen surface that can be achieved through beam-induced scrubbing. Figure 5 (upper) shows the heat load from electron-cloud simulations for a main dipole and quadrupole as a function of bunch intensity and different SEY values, where the multipacting process is modelled as described in [24]. A SEY of 1.3 is sufficient to fully suppress the e-cloud in dipoles, while much lower values are needed for the quadrupoles, hardly achievable by beam-induced scrubbing. Although the LHC is being operated with 25 ns bunch spacing, accumulating a significant electron dose on the beam screen surfaces, to-date a significant heat load from electron cloud is still measured on the arc beam screens. In case a sufficiently low SEY cannot be achieved, e-cloud effects can be mitigated by using specially conceived filling patterns. By using the flexibility of the injector complex, bunch trains with long enough gaps interspersed, to prevent the build-up of electron cloud along the ring circumference, can be built. An alternative scenario (referred to as 8b+4e [25]) based on very short trains with 25 ns spacing has been conceived to reduce e-cloud effects in the HL-LHC and has been considered as part of the HL-LHC operational scenarios. Although the effectiveness of the 8b+4e scheme for electron cloud suppression has been proven in the LHC in 2015 [26], it should be stressed that the integrated luminosity provided by this special filling scheme is reduced by about 25 %, which justify the choice of beam scrubbing as the baseline for e-cloud mitigation strategy.

Figure 5 (lower) shows the heat load expected from electron cloud along the triplet assemblies at the high-luminosity IPs. It can be noticed that the least efficient multipacting (lower heat load) occurs at the locations of the long-range encounters (vertical dashed lines) and that the heat load in the D1 dipole is comparable to that in the quadrupoles.

Surface treatments, such as amorphous carbon coating, are foreseen on the beam screens of the triplet and D1 magnet assemblies for all experimental insertions to achieve a SEY of 1.1 or lower (these technologies are presently being validated at the COLDEX experiment at the SPS). This condition will lead to heat loads from e-cloud of approximately 150 to 200 W per triplet or
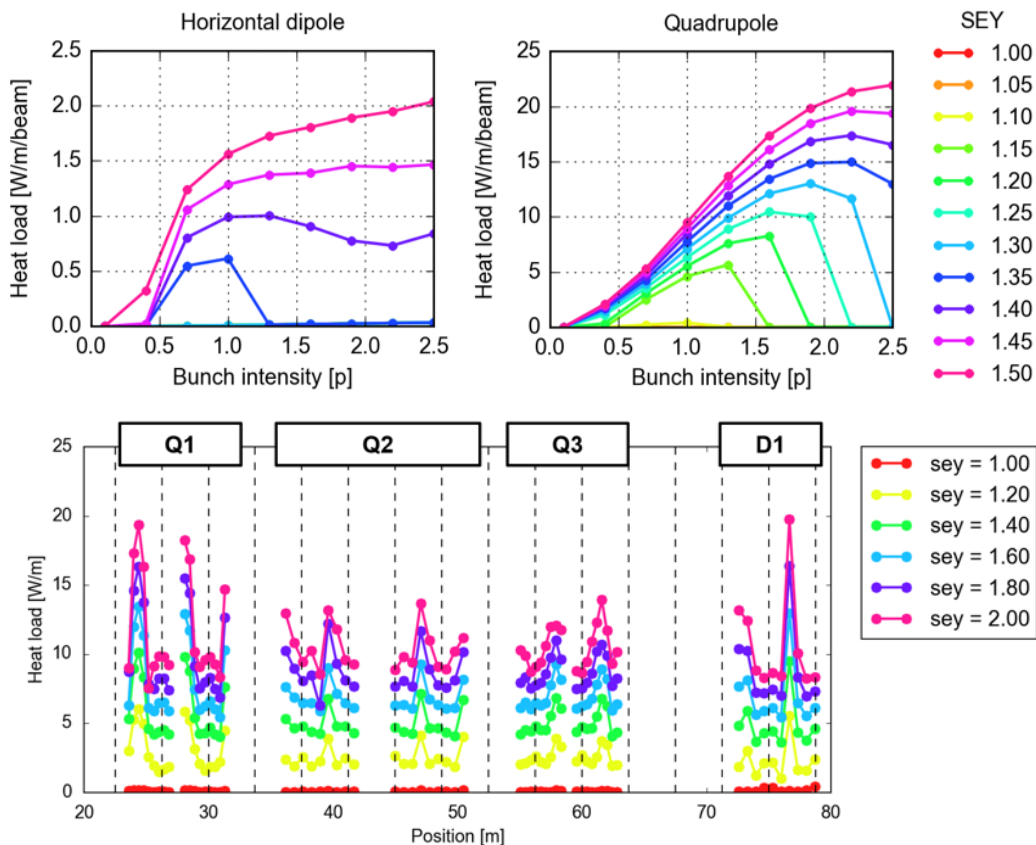
Figure 5. Upper: simulated heat load from e-cloud in the arc magnets as a function of bunch intensity and SEY. Lower: simulated heat load from e-cloud along the triplet and D1 magnets in IR1 and 5 for HL-LHC beam parameters. The vertical dashed lines indicate the locations of the long-range encounters.

lower. The heating mechanisms for the beam screens of the twin-bore cold magnets have been studied in detail and the estimated thermal loads for all the insertion regions are reported in [27]. The present baseline includes the surface treatment of the beam screens of the elements installed in the matching section of the high-luminosity IPs (D2, Q4, Q5, and associated correctors). The need of coating additional elements is being assessed, taking into account the heat load estimates and the available cryogenic power during the HL-LHC era [3]. The above estimates rely strongly on the SEY dependence on the electron energy [24] that determines, e.g., the scaling of the heat load on the bunch population. The experimental confirmation of these simulations with bunch intensities close to the nominal for HL-LHC, which will become available after the implementation of the LIU Project [28] in 2021, is vital for the validation of the HL-LHC performance.

3.4 Cleaning and collimation

The HL-LHC beams, with stored energy over 700 MJ, are highly destructive, and for this a multistage collimation system has been installed [1, 29] to safely dispose of beam losses. Unlike other high-energy colliders, the LHC and the HL-LHC require efficient beam collimation during all stages of operation, from injection to collision energy.

The two-fold increase in stored beam energy for HL-LHC baseline parameters will require a significant improvement of cleaning performance. Material robustness and beam impedance are critical points in view of HL-LHC operation, together with reduction of collimator setup time and maximisation of system availability, which are essential for achieving the HL-LHC design goals.

To meet with the new requirements, the HL-LHC collimation system builds on the current one, with several upgrades. The backbone of the HL-LHC collimation will remain the betatron (IR7) and momentum (IR3) cleaning systems installed in two separated insertions [1]. A three-stage system, based on primary (TCP), secondary (TCS), and on shower absorber (TCLA) collimators, is deployed in these insertions. In all experimental insertions, tertiary (TCT) collimators are installed to protect the triplet and the Q4 and Q5 magnets from incoming beam losses. Physics debris (TCL) collimators are installed downstream of the high-luminosity interaction points to protect matching section and dispersion suppressor magnets from the collision products. Including also injection and dump protection devices, the present system counts a total of 92 movable devices.

The system already underwent an important upgrade during LS1, when beam position monitors were successfully deployed in 18 new collimators [30, 31] for faster alignment and continuous orbit measurements. This new functionality is now the baseline for each new HL-LHC collimators.

The planned upgrades address limitations encountered both for proton and heavy-ion beam operation [2]:

- Addition of one dispersion suppressor collimator (TCLD) per beam and side of IR7 to improve the betatron cleaning performance for ion and proton beams [32–34]. This collimator, installed in cell 8, will intercept dispersive losses of halo particles that have interacted with the primary collimators. The space for installing a warm collimator is made available by replacing a standard 8.33 T, Nb-Ti LHC main dipole with 2 new 11 T, Nb$_3$Sn dipoles [3, 35].

- Addition of one dispersion suppressor collimator (TCLD) per beam and side of IR2 to intercept the products of Pb-Pb collisions that would otherwise quench dispersion suppressor magnets [36–38]. The TCLD will be installed in the interconnection cryostat and will not require any 11 T dipole unit.

- Replacement of all secondary collimators in IR7 with a new design with lower impedance, to ensure the stability of the HL-LHC beams. The present baseline foresees using Mo-Gr (molybdenum-graphite) devices [39] coated with a pure Mo, 5 μm-thick layer. This material showed comparable robustness against beam impacts as the present carbon-based secondary collimators [39], but has an electrical resistivity 5 (uncoated) to 100 times (coated) smaller.

- Complete re-design of the high-luminosity IRs, for protection against incoming beam losses and for cleaning of collision products. For each IR and beam, two pairs of vertical and horizontal tertiary collimators will be installed upstream of the IP; three collimators and three fixed masks will be installed downstream of the IP to protect magnets from physics debris. New, more robust materials are needed to handle beam losses of the ultra-bright HL-LHC beams, in particular in case of fast beam failures that would otherwise risk to damage these collimators [40].

New solutions to improve further the collimation performance are under study. Hollow electron lenses are considered as a possible way to mitigate beam loss spikes at the HL-LHC, through the

active control of halo population and diffusion speed [41]. Crystal collimation is also being studied as a means to improve cleaning efficiency. Following the successful demonstration of channelling of 6.5 TeV protons, obtained in 2015 with a test stand installed in IR7 [42], crystal collimation is now considered as a promising option to improve cleaning efficiency for ion beams at the HL-LHC.

4 Conclusions and outlook

The design of the high luminosity LHC upgrade underwent already a number of changes and considerable evolution since its inception, and in summer 2016 a a major milestone was achieved, when an in-depth re-baselining of the whole Project took place.

The future runs of the LHC will be crucial for the confirmation of the design choices made for the HL-LHC as the LHC could be used as test bed for the most challenging techniques needed for the HL-LHC, e.g., the deployment of the ATS optics. The experience gained in the LHC operation might lead to further adjustments of the set of beam parameters and running scenarios.

Since crab cavities have yet to be realised and used in hadron rings, beam tests with a prototype are a prerequisite to identifying potential risks from the technology to safe and reliable operation of the HL-LHC. Therefore, an essential milestone is a crab cavity test in the CERN Super Proton Synchrotron (SPS), with the aim of demonstrating the operational reliability, ensuring machine protection, and cavity transparency. The beam tests are planned as machine development studies during the run 2018 and the successful validation of the crab cavities in the SPS is a prerequisite for installation in the LHC ring.

References

[1] O. Brüning et al. eds., *LHC design report vol.* 1, CERN-2004-003-V-1, CERN, Geneva Switzerland (2004).

[2] O. Brüning et al. eds., *The High Luminosity Large Hadron Collider*, World Scientific, Singapore (2015).

[3] G. Apollinari et al. eds., *High-Luminosity Large Hadron Collider (HL-LHC): preliminary design report*, CERN-2015-005, CERN, Geneva Switzerland (2015).

[4] G. Apollinari et al. eds., *High-Luminosity Large Hadron Collider (HL-LHC) technical design report V*.01, in publication.

[5] L. Medina and R. Tomás, *Performance and operational aspects of HL-LHC scenarios*, in *Proc. IPAC*16, K.S. Kim et al. eds., (2016).

[6] S. Fartoukh, *Achromatic telescopic squeezing scheme and application to the LHC and its luminosity upgrade*, *Phys. Rev. ST Accel. Beams* **16** (2013) 111002.

[7] S. Fartoukh, *First demonstration with beam of the Achromatic Telescopic Squeezing (ATS) scheme*, in *Proc. Chamonix* 2012 *Workshop on LHC Performance*, C. Carli ed., CERN-2012-006, (2012), pg. 128.

[8] E. Métral et al., *Measurement and interpretation of transverse beam instabilities in the CERN Large Hadron Collider (LHC) and extrapolations to HL-LHC*, in *Proc. HB*2016 *Workshop*, D. Gous et al. eds., CERN-ACC-2016-0098, (2016), pg. 254.

[9] G. Arduini, *Potential performance reach for the HL-LHC in case of a depleted beam halo*, in *Review of the needs for a hollow e-lens for the HL-LHC*, CERN, Geneva Switzerland October 6–7 2016.

[10] M. Schenk et al., *Use of RF quadrupole structures to enhance stability in accelerator rings*, in *Proc. HB*2016 *Workshop*, D. Gous et al. eds., CERN-ACC-2016-0096, (2016), pg. 505.

[11] K. Li et al., *Do we need a wide-band transverse feedback in the LHC/HL-LHC?*, in 75th *HiLumi WP2 meeting*, August 23 2016.

[12] W. Herr, *Observations of beam-beam effects in the LHC in* 2011, in *Proc. Chamonix* 2012 *Workshop on LHC Performance*, C. Carli ed., CERN-2012-006, (2012), pg. 99.

[13] Y. Luo and F. Schmidt, *Dynamic aperture studies for LHC optics version* 6.2 *at collision*, LHC-PROJECT-NOTE-310, CERN, Geneva Switzerland (2003).

[14] A. Valishev, Yu. Alexahin, V. Lebedev and D. Shatilov, *Simulation of beam-beam effects and Tevatron experience*, 2012 *JINST* **7** P12002 [arXiv:0906.0386].

[15] K. Ohmi, *Beam-beam effects under the influence of external noise*, in *Proc. ICFA Mini-Workshop on Beam-Beam Effects in Hadron Colliders*, W. Herr and G. Papotti eds., CERN-2014-004, (2014), pg. 69 [arXiv:1410.4092].

[16] J. Qiang, J. Barranco and K. Ohmi, *Beam-beam simulation of crab cavity white noise for LHC upgrade*, in *Proc. IPAC*15, S. Henderson et al. eds., (2015), pg. 2206.

[17] J. Qiang et al., *A parallel particle-in-cell model for beam-beam interaction in high energy ring colliders*, *J. Comput. Phys.* **198** (2004) 278.

[18] T. Pieloni, *A study of beam-beam effects in hadron colliders with a large number of bunches*, Ph.D. thesis, CERN-THESIS-2010-056, EPFL, Lausanne Switzerland (2008).

[19] J. Qiang et al., *Strong-strong beam-beam simulation for LHC upgrade*, in *Proc. IPAC*14, G. Arduini et al. eds., (2014), pg. 1006.

[20] A. Valishev et al., 42nd *HiLumi WP2 Task Leader Meeting*, CERN, Geneva Switzerland March 6 2015.

[21] Y. Papaphilippou et al., 6th *HL-LHC collaboration meeting*, Paris France November 14–16 2016.

[22] S. Fartoukh et al., *Compensation of the long-range beam-beam interactions as a path towards new configurations for the High Luminosity LHC*, *Phys. Rev. ST Accel. Beams* **18** (2015) 121001.

[23] A. Valishev et al., *Preliminary estimates of beam-beam effects*, HiLumi LHC Milestone report CERN-ACC-2014-0066, CERN, Geneva Switzerland (2014).

[24] R. Cimino et al., *Can low-energy electrons affect high-energy physics accelerators?*, *Phys. Rev. Lett.* **93** (2004) 014801.

[25] H. Damerau et al., *LIU: exploring alternative ideas*, in *Proc. Review of LHC and Injector Upgrade Plans Workshop (RLIUP)*, B. Goddard and F. Zimmermann eds., CERN-2014-006, (2014), pg. 127.

[26] G. Iadarola et al., *Performance limitation from electron cloud in* 2015, in *Proc.* 6th *Evian Workshop on LHC beam operation*, B. Goddard and S. Dubourg eds., CERN-ACC-2015-376, (2015), pg. 101.

[27] G. Iadarola et al., *Expected heat load for the two bore magnets in the IRs of the HL-LHC*, CERN-ACC-2016-0112, CERN, Geneva Switzerland (2016).

[28] H. Damerau et al. eds., *LHC injectors upgrade, technical design report, vol. I: protons*, CERN-ACC-2014-0337, CERN, Geneva Switzerland (2014).

[29] R. Assmann et al., *The final collimation system for the LHC*, in *Proc. EPAC* 2006, J. Poole and C. Petit-Jean-Genaz eds., Edinburgh Scotland (2006), pg. 986.

[30] A. Dallocchio et al., *LHC collimators with embedded beam position monitors: a new advanced mechanical design*, in *Proc. IPAC*11, C. Petit-Jean-Genaz ed., CERN-ATS-2011-228, (2011), pg. 1611.

[31] D. Wollmann et al., *Beam feasibility study of a collimator with in-jaw beam position monitors*, *Nucl. Instrum. Meth.* **A 768** (2014) 62.

[32] R. Bruce, A. Marsili and S. Redaelli, *Cleaning performance with 11 T dipoles and local dispersion suppressor collimation at the LHC*, in *Proc. IPAC*14, G. Arduini et al. eds., (2014), pg. 170.

[33] A. Marsili, R. Bruce and S. Redaelli, *Collimation cleaning for HL-LHC optics scenarios with error models*, in *Proc. IPAC*14, G. Arduini et al. eds., (2014), pg. 163.

[34] A. Lechner et al., *Power deposition in LHC magnets with and without dispersion suppressor collimators downstream of the betatron cleaning insertion*, in *Proc. IPAC*14, G. Arduini et al. eds., (2014), pg. 112.

[35] D. Ramos et al., *Integration of the 11 T Nb$_3$Sn dipoles and collimators in the LHC*, *IEEE Trans. Appl. Supercond.* **26** (2016) 3800105.

[36] R. Bruce et al., *Beam losses from ultra-peripheral nuclear collisions between $^{208}Pb^{82+}$ ions in the Large Hadron Collider and their alleviation*, *Phys. Rev. ST Accel. Beams* **12** (2009) 071002.

[37] M. Schaumann, *Heavy-ion performance of the LHC and future colliders*, Ph.D. thesis, CERN-THESIS-2015-195, RWTH Aachen, Aachen Germany (2015).

[38] J.M. Jowett et al., *Bound-free pair production in LHC Pb-Pb operation at 6.37 Z TeV per beam*, in *Proc. IPAC*16, K.S. Kim et al. eds., CERN-ACC-2016-245, (2016), pg. 1497.

[39] E. Quaranta et al., *Towards optimum material choices for the HL-LHC collimator upgrade*, in *Proc. IPAC*16, K.S. Kim et al. eds., CERN-ACC-2016-0062, (2016), pg. 2498.

[40] R. Bruce, R.W. Assmann and S. Redaelli, *Calculations of safe collimator settings and beta* at the CERN Large Hadron Collider*, *Phys. Rev. ST Accel. Beams* **18** (2015) 061001.

[41] S. Redaelli et al., *Plans for deployment of hollow electron lenses at the LHC for enhanced beam collimation*, in *Proc. IPAC*15, S. Henderson et al. eds., CERN-ACC-2015-370, (2015), pg. 2462.

[42] W. Scandale et al., *Observation of channeling for 6500 GeV/c protons in the crystal assisted collimation setup for LHC*, *Phys. Lett.* **B 758** (2016) 129.